Title

Sex-dependent changes in metabolism and behavior, as well as reduced anxiety after eliminating ventromedial hypothalamus excitatory output

Journal

Molecular Metabolism, 4(11)

ISSN

2212-8778

Authors

Cheung, Clement C

Krause, William C

Edwards, Robert H

et al.

Publication Date

2015-11-01

DOI

10.1016/j.molmet.2015.09.001

Peer reviewed

Original article

MOLECULAR METABOLISM

Sex-dependent changes in metabolism and behavior, as well as reduced anxiety after eliminating ventromedial hypothalamus excitatory output

Clement C. Cheung [1,4,5], William C. Krause [1,4], Robert H. Edwards [2], Cindy F. Yang [3], Nirao M. Shah [3], Thomas S. Hnasko [2,6], Holly A. Ingraham [1,*]

ABSTRACT

Objectives: The ventromedial hypothalamic nucleus (VMH) regulates energy homeostasis as well as social and emotional behaviors. Nearly all VMH neurons, including those in the sexually dimorphic ventrolateral VMH (VMHvl) subregion, release the excitatory neurotransmitter glutamate and use the vesicular glutamate transporter 2 (Vglut2). Here, we asked how glutamatergic signaling contributes to the collective metabolic and behavioral responses attributed to the VMH and VMHvl.

Methods: Using *Sf1-Cre* and a *Vglut2* floxed allele, *Vglut2* was knocked-out in SF-1 VMH neurons ($Vglut2^{Sf1\text{-}Cre}$). Metabolic and neurobehavioral assays were carried out initially on $Vglut2^{fl/fl}$ and $Vglut2^{Sf1\text{-}Cre}$ mice in a mixed, and then in the C57BL/6 genetic background, which is prone to hyperglycemia and diet induced obesity (DIO).

Results: Several phenotypes observed in $Vglut2^{Sf1\text{-}Cre}$ mice were largely unexpected based on prior studies that have perturbed VMH development or VMH glutamate signaling. In our hands, $Vglut2^{Sf1\text{-}Cre}$ mice failed to exhibit the anticipated increase in body weight after high fat diet (HFD) or the impaired glucose homeostasis after fasting. Instead, there was a significant sex-dependent attenuation of DIO in $Vglut2^{Sf1\text{-}Cre}$ females. $Vglut2^{Sf1\text{-}Cre}$ males also display a sex-specific loss of conditioned-fear responses and aggression accompanied by more novelty-associated locomotion. Finally, unlike the higher anxiety noted in $Sf1^{Nestin\text{-}Cre}$ mice that lack a fully formed VMH, both male and female $Vglut2^{Sf1\text{-}Cre}$ mice were less anxious.

Conclusions: Loss of VMH glutamatergic signaling sharply decreased DIO in females, attenuated aggression and learned fear in males, and was anxiolytic in males and females. Collectively, our findings demonstrate that while glutamatergic output from the VMH appears largely dispensable for counter regulatory responses to hypoglycemia, it drives sex-dependent differences in metabolism and social behaviors and is essential for adaptive responses to anxiety-provoking stimuli in both sexes.

Keywords VMH; VGlut2; Sex-dependent obesity; Excitatory output; Anxiety; Male aggression

1. INTRODUCTION

The murine ventromedial hypothalamus (VMH) is molecularly and functionally complex as evidenced by gene expression patterns [1] and phenotypes arising from numerous genetic lesions. Physiological and behavioral functions associated with the VMH include metabolic homeostasis, reproduction, social behaviors, anxiety, and female-specific energy expenditure, all of which are presumably mediated by distinct VMH neuronal subpopulations. Although complete annotation of these functionally distinct VMH neuronal subsets has yet to emerge, nearly all VMH neurons express two markers, steroidogenic factor 1 (SF-1 encoded by *Nr5a1*), and the vesicular glutamate transporter 2 (VGLUT2 encoded by *Slc17a6*). The prominent expression of *Vglut2* in the VMH [2,3] suggests that excitatory, glutamatergic neurotransmission mediates multiple and diverse aspects of VMH functions. In addition, glutamatergic connections between the VMH and other metabolic brain centers, such as the arcuate nucleus have been documented [4,5]

To date, numerous genetic perturbations of the VMH have been reported, which target either VMH development or general signaling components affecting metabolism. For example, disrupting VMH

[1]Department of Cellular and Molecular Pharmacology, Mission Bay Campus, University of California, San Francisco 94143, United States [2]Department of Physiology and Neurology, Mission Bay Campus, University of California, San Francisco 94143, United States [3]Department of Anatomy, Mission Bay Campus, University of California, San Francisco 94143, United States

[4] Clement C. Cheung and William C. Krause contributed equally to this work.

[5] Present address: Department of Pediatrics, Center for Endocrinology, Diabetes, and Metabolism, Children's Hospital Los Angeles, University of Southern California, Los Angeles, CA 90027, United States.

[6] Present address: University of California, San Diego, Department of Neurosciences, 9500 Gilman Drive, La Jolla, CA 92093, United States.

*Corresponding author. E-mail: holly.ingraham@ucsf.edu (H.A. Ingraham).

Received July 20, 2015 • Revision received August 26, 2015 • Accepted September 2, 2015 • Available online 11 September 2015

http://dx.doi.org/10.1016/j.molmet.2015.09.001

development by reducing or ablating SF-1 prenatally leads to obesity in both sexes on standard chow and accelerates diet-induced obesity (DIO) on high fat diet (HFD) [6–8]. Eliminating SF-1 postnatally, using the *CamKII-Cre* preserves the gross architecture of the VMH, but still promotes DIO as well as hyperglycemia in both fed and fasted states [6]. We previously reported that blocking development and migration of neurons to the sexually dimorphic ventrolateral VMH (VMHvl) subregion results in marked female-specific obesity on standard chow [9]. Several genetic lesions in SF-1 expressing neurons that manipulate metabolic signaling pathways are also reported to change DIO in both sexes. Reducing leptin sensitivity after deleting *LepR, Pl3K* (p110α), or *Ptpn1* with the *Sf1-Cre* increases susceptibility to DIO [10–13]. On the other hand, deleting insulin signaling (*Insr*) using the same *Sf1-Cre* prevents insulin-mediated inhibition of VMH neuronal activity and decreases DIO, at least in males [14]. Whether loss of these general signaling components in other SF-1 expressing tissues contributes to the observed metabolic phenotypes remains unclear. It is also unclear whether disrupting excitatory neurotransmission from all VMH neurons recapitulates the selective genetic lesions described above and leads to increased food intake and DIO. Tong et al. previously generated a VMH knockout of *Vglut2* using *Sf1-Cre* ($Vglut2^{Sf1\text{-}Cre}$) in a mixed genetic background [15]. Surprisingly, only a modest increase in weight gain is observed in $Vglut2^{Sf1\text{-}Cre}$ males and females in response to a high-sucrose, high-fat diet (58% kcal fat). However, mutant mice exhibit lowered serum glucose in the fasted but not fed state, suggesting that loss of VMH excitatory output blunts the counterregulatory response to hypoglycemia.

As mentioned above, the VMH also regulates fear and anxiety-like behaviors [16–18] as well as social behaviors that are regulated by the VMHvl, such as male aggression [19–21]. Inhibiting SF-1 neurons via pharmacogenetics decreases freezing to predator stimuli in both males and females, suggesting that the VMH is required for mounting appropriate defensive behaviors in both sexes [17]. In a CNS-specific knockout of SF-1 using the *Nestin-Cre* ($Sf1^{Nestin\text{-}Cre}$), anxiety-like behaviors are elevated as evidenced by fewer entries and less time spent in the open arm in the elevated plus-maze (EPM) assay [18]. However, as with the global $Sf1^{-/-}$ knockout, $Sf1^{Nestin\text{-}Cre}$ mice show gross abnormalities in VMH architecture. Hence, it is unclear if the increased anxiety phenotype noted in the $Sf1^{Nestin\text{-}Cre}$ mice arises from organizational rather than functional VMH deficits.

To assess how blocking all excitatory VMH output might modulate the many physiological and behavioral functions associated with the VMH, we recreated the $Vglut2^{Sf1\text{-}Cre}$ allele using *Sf1-Cre* and a *Vglut2* floxed allele ($Vglut2^{fl/fl}$) [22]. As shown previously, targeted deletion of *Vglut2* effectively blocks all synaptic release of glutamate from neurons that express this transporter protein [23]. Using multiple metabolic and behavioral assays, we examined the consequences of silencing glutamatergic signaling in both male and female mice bred in two genetic backgrounds. Analyses of these $Vglut2^{Sf1\text{-}Cre}$ mice show that excitatory VMH output is an important factor in female metabolism, but surprisingly, less so for glucose homeostasis. Further, our results establish an essential role for VMH glutamatergic output in mounting adaptive behavioral responses to contextual and social cues.

2. MATERIALS & METHODS

2.1. Animals

$Vglut2^{+/fl}$ mice in a mixed C57BL/6, Sv129J background were provided by Dr. R.D. Palmiter, (University of Washington) [22]. $Sf1^{+/Cre}$ mice were provided by Dr. J.K. Elmquist (University of Texas Southwestern Medical Center) [11] and subsequently backcrossed into the C57BL/6 background (Taconic Biosciences), which was confirmed by microsatellite analysis. $Vglut2^{fl/fl}$ mice were generated and maintained on a mixed background or backcrossed for 10 generations into the C57BL/6 background. Experimental cohorts were obtained by crossing $Sf1^{+/Cre}$; $Vglut2^{fl/fl}$ with $Vglut2^{fl/fl}$ mice. We previously generated and characterized the $Sf1^{TauGFP}$ reporter mice [24].

Mice were maintained on a 12 h light–dark cycle with *ad libitum* access to water and to either a standard chow diet (5058; LabDiet, 4% fat) or a high fat diet (D12492; Research Diets, 60% fat), as indicated. All animal procedures were performed in accordance with the UCSF animal care committee's regulations and the Ingraham lab IACUC protocol of record.

2.2. Tissue collection and processing

Mice were deeply anesthetized with 2.5% Avertin and perfused with phosphate buffered saline (PBS) followed by 4% paraformaldehyde (PFA). Brains were dissected and post-fixed overnight in 4% PFA. Fixed tissue was cryoprotected in 30% sucrose and embedded in OCT (Tissue-Tek). Cryosections (20 μm) were collected on glass slides and stored at −80 °C until processing.

2.3. Immunofluorescence and in situ hybridization

Frozen brain sections were processed using standard procedures. Reporter GFP expression was detected by immunofluorescence using chicken anti-GFP antibody (1:2500; Aves Labs) and AlexaFluor 488-conjugated goat anti-chicken antibody (1:1000; Invitrogen). Detection of mRNA expression by in situ hybridization (ISH) was accomplished using probes against the carboxy-termini and 3′ UTR of *Vglut1* and *Vglut3* (nt:1589–2510 and nt:1511–1869, respectively); exon 2 of *Vglut2* (nt:902–1230); and exons 9–18 of *Gad67* (nt:1313–2267). DIG-labeled (Roche) riboprobes were transcribed according to the manufacturers specifications. ISH was performed using standard procedures, as previously described [1].

Double-label immunofluorescence in situ hybridization (DISH) was performed with the following modifications to standard IF/ISH protocols. Sections were permeabilized with 0.3% Triton X-100 (in PBS) for 10 min at room temperature. *Vglut2* riboprobe was hybridized to the sections overnight at 72 °C. Sections were washed and blocked with 10% heat-inactivated donkey serum (HIDS) in buffer B1 (0.1 M Tris, pH 7.5; 0.15 M NaCl) for 3 h at room temperature. Primary antibodies (1:3000 Anti-Dig-AP, Roche; 1:2500 chicken anti-GFP) diluted in B1 with 1% HIDS were added to the sections and incubated overnight at 4 °C. Sections were washed and incubated with biotin-conjugated goat anti-chicken antibody (1:500) (Invitrogen) in B1 with 2% HIDS for 2 h at room temperature. After washing 3 × 5 min in buffer TNT (1 M Tris HCl, pH7.5; 5 M NaCl; 0.05% Tween 20), IF and ISH signals were detected sequentially using the TSA Biotin System (Perkin Elmer) and the HNPP Fast Red Detection Kit (Roche), respectively, according to the manufacturers' instructions. Sections were counter-stained with DAPI (1:1000) for 5 min at room temperature and mounted with aqueous mounting media.

2.4. Metabolic analyses

Male and female body weights were recorded weekly beginning at the time of weaning (3 wks of age). Fed and 24-hour fasting glucose levels were measured in 8–10 wk old mice on standard chow or after 6 wks on HFD. Glucose tolerance tests were performed after 6 wks on HFD. Mice were fasted overnight for 16 h and given glucose (2 g/kg) by IP injection. For both assays, blood was collected from the tail vein, and glucose levels measured using the OneTouch Ultra Glucometer (LifeScan).

Measurements of metabolic parameters and indirect calorimetry were conducted by the UCSF Diabetes Center Metabolic Core facility using

the Oxymax Comprehensive Laboratory Animal Monitoring System (CLAMS) chambers. Prior to data collection, mice were acclimated to individual housing for 1 wk and subsequently acclimated to CLAMS chambers for 3 days. Chambers were maintained at room temperature, and mice had *ad libitum* access to standard chow and water.

2.5. Behavioral analyses

Levels of anxiety in adult male and female mice were analyzed by the UCSF Gladstone Mouse Phenotyping Core Facility (http://labs.gladstone.ucsf.edu/behavioral/home). For all assays described below, adult $Vglut2^{Sf1\text{-}Cre}$ and $Vglut2^{fl/fl}$ control littermates in the C57BL/6 background were used. Tests were started during the light phase between 9:00—11:00. Mice were allowed to recover for at least 1 week between each test. The order of testing for each experimental cohort is as follows:

2.6. Rotarod

Subjects were transferred to the room containing the rotarod apparatus 30 min prior to testing. During the test, the speed of the rotating rod was increased from 4 to 40 rpm at 8 rpm/min. Latency to fall was recorded by the experimenter. Vertical spacers on the rod allowed five mice to be tested simultaneously. Each mouse was tested 3 times with an inter-trial interval of 15—20 min. The rotarod was cleaned with 70% ethanol between testing sessions.

2.7. Open field assay

The arena was a clear plastic chamber (41 $\times$ 41 $\times$ 30 cm). Activity and position measurements in the arena were recorded electronically using two 16 $\times$ 16 photobeam arrays (San Diego Instruments). Mice were habituated to the testing room under normal light for 30 min. During the testing interval, mice were allowed to explore the arena for 15 min. The arena was cleaned with 70% ethanol between testing sessions.

2.8. Elevated plus-maze

The testing apparatus consisted of a plus-shaped maze (Hamilton—Kinder) with two open and two closed arms positioned 63 cm above the ground. Mice were transferred to the testing room and acclimated to dim lighting for 30 min. At the start of the test, subjects were placed in the intersection of the plus-maze. Mice were allowed to explore the maze for 10 min, while activity and location measurements were recorded electronically. The maze was cleaned with 70% ethanol between testing sessions.

2.9. Corticosterone assay

Tail vein blood was collected in the beginning of the light phase to determine baseline corticosterone levels in control and mutant mice. The following day, an acute stress was induced by 15 min of restraint in the Broome Rodent Restrainer (Harvard Apparatus) or by a 5 min exposure to the elevated plus-maze. Following these stressors, a second blood sample was collected. Plasma hormone levels were quantified using the Corticosterone Enzyme Immunoassay (EIA) Kit (Cayman Chemical), according to the manufacturer's instructions.

2.10. Cued fear conditioning

Training and testing were performed in a sound attenuated clear, square chamber. Mice were transferred to the room containing the conditioning apparatus 30 min before training or testing. Initial levels of freezing were recorded of 5 min with no audible tone or shock presented. The next day, 3 min baseline freezing levels were recorded. The mice were then trained with three repetitions of a 30 s audible tone co-terminating with a 2 s foot shock. After each training trial, freezing levels were recorded for 90 s. On day 3, the context of the conditioning apparatus was altered (switched to a black, triangular, unlit chamber). After 2.5 min in the chamber, mice were presented with three 30 s exposures to the conditioned tone (100 s inter-tone interval). Freezing levels during each 30 s tone exposure were recorded.

2.11. Predator odor assay

Experimental mice were habituated to testing environment for 45 min prior to exposure of 30 μL of 10% solution of 2,3,5-Trimethyl-3-thiazoline (TMT) (Sigma) placed on filter paper. Behaviors were videotaped in the dark cycle with red light while the experimenter was out of room. Total exposure was 5 min, and responses scored for the final 3 min. Time spent engaged in freezing, sniffing, and grooming were scored by an observer, who was blinded to the genotype of mice.

2.12. Resident intruder assay

Experimental mice were singly housed for 1 wk. Individual males from a socially housed cohorts were placed into the home cages of the resident $Vglut2^{fl/fl}$ and $Vglut2^{Sf1\text{-}Cre}$ male mice, and mice were allowed to interact for 15 min. Interactions were videotaped and scored offline. Attacks toward the intruder were scored twice by 2 independent observers, who were blinded to the genotype of mice.

2.13. Statistics

Data were analyzed using the GraphPad Prism statistical software package (version 6.0). Pairwise comparisons were made using unpaired, two-tailed *t*-tests. Comparisons involving multiple factors were made using 2-way ANOVA with repeated measures and Bonferroni post-test. Results were considered statistically significant when $p < 0.05$. Data are presented as means $\pm$ SEM. For all figures, * $= p < 0.05$, ** $= p < 0.01$, *** $= p < 0.005$, and **** $= p < 0.001$.

3. RESULTS

3.1. Loss of *Vglut2* expression in $Vglut2^{Sf1\text{-}Cre}$ mice does not alter gross organization of the VMH

As expected, SF-1 and *Vglut2* are coexpressed throughout the rodent VMH (Figure 1A). We used *Sf1-Cre* backcrossed into a pure C57BL/6 background [11,24] and $Vglut2^{fl/fl}$ [22,25] to conditionally eliminate VGLUT2 in neurons from the SF-1 lineage ($Vglut2^{Sf1\text{-}Cre}$). As demonstrated previously, eliminating exon 2 renders VGLUT2 non-functional [23]. Within the CNS, *Sf1-Cre*-mediated loss of *Vglut2* is selective for the VMH and does not diminish *Vglut2* expression in other brain regions (Figure 1B). Furthermore, no compensatory upregulation of the other vesicular glutamate transporters, *Vglut1* or *Vglut3* is observed in the VMH of $Vglut2^{Sf1\text{-}Cre}$ mice. Similarly, $Vglut2^{Sf1\text{-}Cre}$ males and females show normal patterns of glutamate decarboxylase (*Gad67*) expression, which marks inhibitory neurons and is normally excluded from the VMH (Figure 1B). No differences in the pattern and intensity of major VMH projections were noted in $Vglut2^{Sf1\text{-}Cre}$, as illustrated by the prominent ascending fibers through the ventral supraoptic commissure (VSOC) (Figure 1C) [24]. Taken together, these data establish that the gross exterior boundaries and major efferent projections of the VMH remain intact after deleting *Vglut2* in the VMH.

3.2. Eliminating *Vglut2* in the VMH does not change fasting blood glucose and unexpectedly attenuates diet-induced obesity in females

Control and mutant mice were initially maintained in a mixed genetic background. When fed standard chow (4% kcal fat), no significant differences in body weight were observed between $Vglut2^{fl/fl}$ and

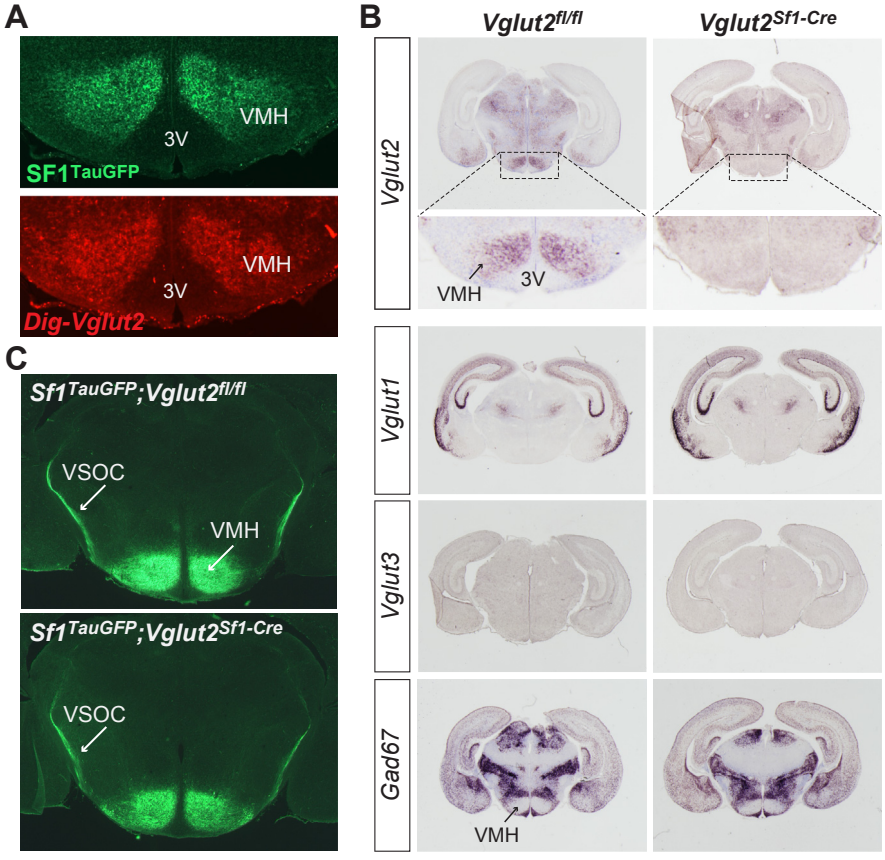

Figure 1: Deletion of *Vglut2*$^{fl/fl}$ in the VMH does not alter gross anatomical organization or lead to compensatory upregulation of Vglut1 or Vglut3. A) SF-1^{+} neurons in the VMH were identified using *Sf1*^{TauGFP}. Expression of the SF-1 reporter (green) and *Vglut2* exon 2 mRNA (red) in coronal sections at the level of the VMH was detected simultaneously using DISH (third ventricle = 3V). **B)** Expression patterns of *Vglut2, Vglut1* and *Vglut3*, as well as *Gad67* transcripts as detected by ISH. For *Vglut2*, higher magnification images of the boxed regions are shown in lower panels. **C)** Coronal sections showing the major VSOC efferent projection from the VMH in *Vglut2*$^{fl/fl}$ (top panel) and mutant *Vglut2*$^{Sf1\text{-}Cre}$ (lower panel) mice. SF-1 neuronal projections are visualized as described in Materials and Methods and after crossing control and mutant mice with *Sf1*^{TauGFP} reporter mice [24].

Vglut2$^{Sf1\text{-}Cre}$ males or females (Figure 2A, left panel). When placed on HFD (60% kcal fat) beginning at 10 wks of age, weight gain was equivalent in *Vglut2*$^{Sf1\text{-}Cre}$ males compared to control littermates (Figure 2B, left panel). *Vglut2*$^{Sf1\text{-}Cre}$ females gained slightly less weight over time on HFD with 2-way repeated measures ANOVA revealing a significant interaction between genotype and time on HFD ($F_{7,98} = 3.116$, $p = 0.0052$). Surprisingly, neither *Vglut2*$^{Sf1\text{-}Cre}$ mutant males nor females exhibited significant differences in fasting blood glucose levels on standard chow or on HFD (Figure 2A, B, right panels). These data differ from the slight increase in DIO and the impaired glucose homeostasis observed in separately derived *Vglut2*$^{Sf1\text{-}Cre}$ mice [15].

Given these discrepant results, we generated congenic *Vglut2*$^{fl/fl}$ and *Vglut2*$^{Sf1\text{-}Cre}$ mice in the C57BL/6 background, a strain that exhibits increased weight gain and hyperglycemia on HFD [26,27]. Similar to the mixed background, body weights between male *Vglut2*$^{Sf1\text{-}Cre}$ and *Vglut2*$^{fl/fl}$ C57BL/6 mice were equivalent on standard chow. However, we observed a modest, but significant, decrease in female *Vglut2*$^{Sf1\text{-}Cre}$ body weights (Figure 3A). Other metabolic parameters were analyzed in *Vglut2*$^{Sf1\text{-}Cre}$ C57BL/6 mice using CLAMS chambers. The decreased weight of *Vglut2*$^{Sf1\text{-}Cre}$ females correlated with a non-significant trend towards increased heat generation during both the light and dark periods (Figure 3B). *Vglut2*$^{Sf1\text{-}Cre}$ females had normal expression of the thermogenic *uncoupling protein 1* (*Ucp1*) in brown adipose tissue (BAT) at both warm and cold temperatures (Figure S1A). Further analysis of the CLAMS data revealed no significant alterations in ambulatory activity, food intake, oxygen consumption, respiratory exchange ratio, or lean mass between female *Vglut2*$^{fl/fl}$ and *Vglut2*$^{Sf1\text{-}Cre}$ mice on standard chow (Figures 3C and S1B).

As expected, DIO was readily apparent in the C57BL/6 mice on HFD compared with the mixed background, especially in females (Figures 3D and 2B). When compared to *Vglut2*$^{fl/fl}$ controls, weight gain in *Vglut2*$^{Sf1\text{-}Cre}$ females was notably lower when placed on HFD at 10 wks of age (Figure 3D); however both genotypes consumed equivalent amounts of HFD (Figure S1C). In contrast, C57BL/6 mutant males showed no body weight differences on HFD. Consistent with the female-specific resistance to DIO, glucose clearance was improved in the *Vglut2*$^{sf1\text{-}Cre}$ females but not in mutant males as measured by an intraperitoneal glucose tolerance test performed at 16 wks of age (Figures 3C and S1D). The unexpected body weight reduction in *Vglut2*$^{Sf1\text{-}Cre}$ females suggests that normal weight gain and sensitivity to DIO in females depends on glutamatergic output from the VMH. It should be noted that no gross deficits in reproduction were noted in *Vglut2*$^{Sf1\text{-}Cre}$ females on both the mixed and C57BL/6 backgrounds, suggesting that the hypothalamic-pituitary-gonad axis controlling reproductive physiology was not impaired in these mutant mice.

3.3. Reduced anxiety-like behaviors in male and female *Vglut2*$^{Sf1\text{-}Cre}$ mice

While conducting metabolic studies in which mice were housed individually, we noted a difference in the location of home cage nests built

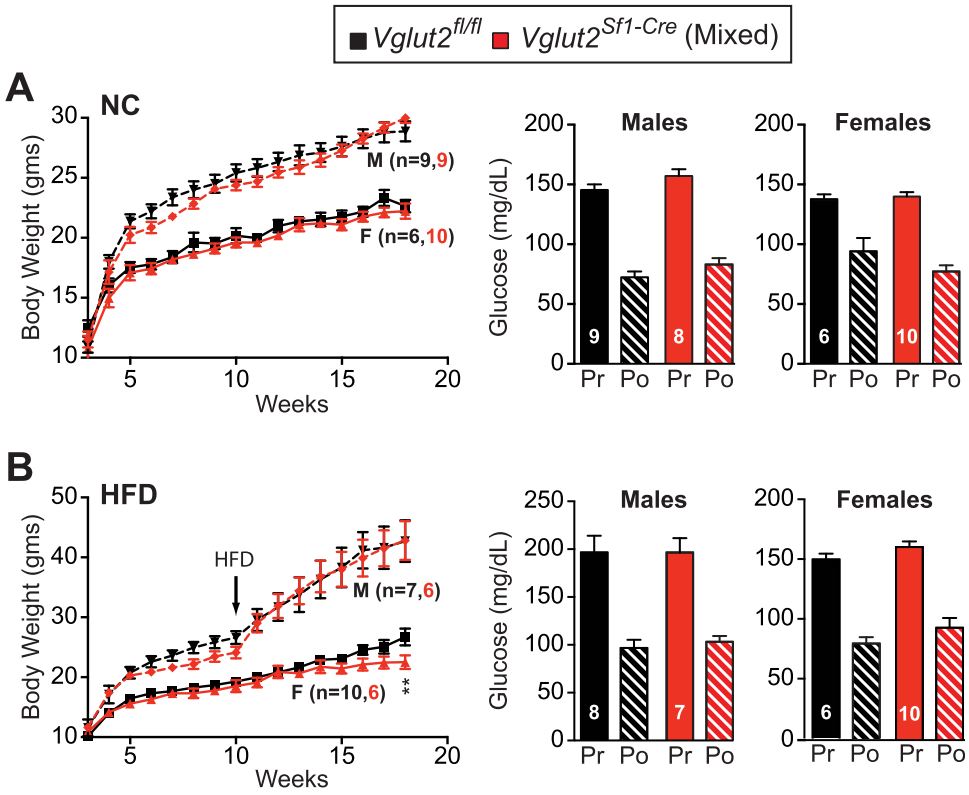

Figure 2: Fasting glucose levels on HFD are unaffected in *Vglut2*$^{Sf1\text{-}Cre}$ on a mixed genetic background. Weekly body weight measurements of male (M) and female (F) *Vglut2*$^{fl/fl}$ and *Vglu2*$^{Sf1\text{-}Cre}$ mice from 3 to 18 weeks of age. **(A)** Body weights of mice on standard chow (left panel) with corresponding blood glucose levels in each cohort measured pre- (Pr, solid bars) and post- (Po, hatched bars) a 24-hour fast (right panel). **(B)** Body weights of mice on standard chow and placed on HFD (arrow) at 10 weeks (left panel) with corresponding blood glucose levels measured as above and after HFD for 6 wks (right panel). Data are presented as means ± SEM. Statistical significance was determined by 2-way repeated measures ANOVA and Bonferroni post-test. Number of animals is indicated in each panel.

by *Vglut2*$^{fl/fl}$ and *Vglut2*$^{Sf1\text{-}Cre}$ mice (Figure 4A). Nearly all *Vglut2*$^{fl/fl}$ control mice (96%) followed a stereotypic pattern and built their nests in the corner of the cage. In contrast, the majority of *Vglut2*$^{Sf1\text{-}Cre}$ mice (62%) chose a central nest location. Based on these preliminary observations, anxiety-like behaviors in mutant and control mice were formally assayed in open field (OF) and elevated plus-maze (EPM) tests. Although the nesting phenotype was initially observed in mutant mice on the mixed background, the following behavioral tests were exclusively performed in C57BL/6 *Vglut2*$^{fl/fl}$ and *Vglut2*$^{Sf1\text{-}Cre}$ mice. The C57BL/6 background is known to have intermediate levels of anxiety-like behavior and therefore allows detection of both anxiolytic and anxiogenic phenotypes [28]. An initial rotarod test confirmed that motor skills were equivalent between genotypes (data not shown). However, in an OF test both male and female *Vglut2*$^{Sf1\text{-}Cre}$ mice exhibited significantly more ambulatory movement in the center of the field than control *Vglut2*$^{fl/fl}$ mice (Figure 4B). We also observed higher total ambulatory activity for *Vglut2*$^{Sf1\text{-}Cre}$ males within the short OF test (15 min) (Figure 4B). Because total ambulatory movement was unchanged in mutant *Vglut2*$^{Sf1\text{-}Cre}$ males when monitored over a 4 day period (Figure S1E), the increased movement in the OF test suggests a greater exploratory drive for mutant males when initially placed in a novel environment.

Exploratory and anxiety-like behaviors were also examined using the EPM assay. Entries into the anxiety-promoting open arm, time spent in the open arm, and distance covered in the open arm were analyzed across two consecutive intervals (0–5 and 5–10 min). Similar to the OF assay, *Vglut2*$^{Sf1\text{-}Cre}$ males, but not females exhibited a higher level of exploratory drive and/or activity in the initial interval (0–5 min), as measured by the total distance traversed in the EPM (Figure 4C, last panel). During the final 5-min interval (5–10 min), both male and female *Vglut2*$^{Sf1\text{-}Cre}$ mice displayed higher levels of all three open arm parameters relative to controls (Figure 4C). Despite the sustained open arm activity observed in mutants, total distance traveled was equivalent between genotypes. A significant interaction between genotype and time was observed for open arm entries (males: $F_{1,22} = 17.33$, $p < 0.0005$; females: $F_{1,25} = 5.751$, $p < 0.05$); this EPM behavior is thought to best reflect altered anxiety levels [29]. The increased open arm activity in the *Vglut2*$^{Sf1\text{-}Cre}$ mice is consistent with their increased time in the center of the OF, and together these results demonstrate that loss of glutamatergic output from the VMH is anxiolytic in both males and females. To confirm that *Vglut2*$^{Sf1\text{-}Cre}$ mice could mount an appropriate physiological response to stressors, serum corticosterone levels were measured after 5 min in the EPM or 15 min of acute restraint. Despite lowered anxiety-like behavior in both the OF and EPM assays, corticosterone levels increased appropriately in *Vglut2*$^{Sf1\text{-}Cre}$ mice (Figure 4D). For both wild type and mutant genotypes, two-way repeated measures ANOVA revealed a significant main effect of stressor only (EPM: $F_{1,21} = 228.8$, $p < 0.0001$; acute restraint: $F_{1,21} = 420.13$, $p < 0.0001$). These data show that the hypothalamic-pituitary-adrenal (HPA) axis is fully intact and unaffected by loss of glutamatergic transmission from the VMH.

3.4. Loss of Vglut2 in the VMH impairs fear conditioning and aggression in males

VMH neurons are part of the circuit linking the amygdala to the periaqueductal grey, both of which are essential for eliciting normal

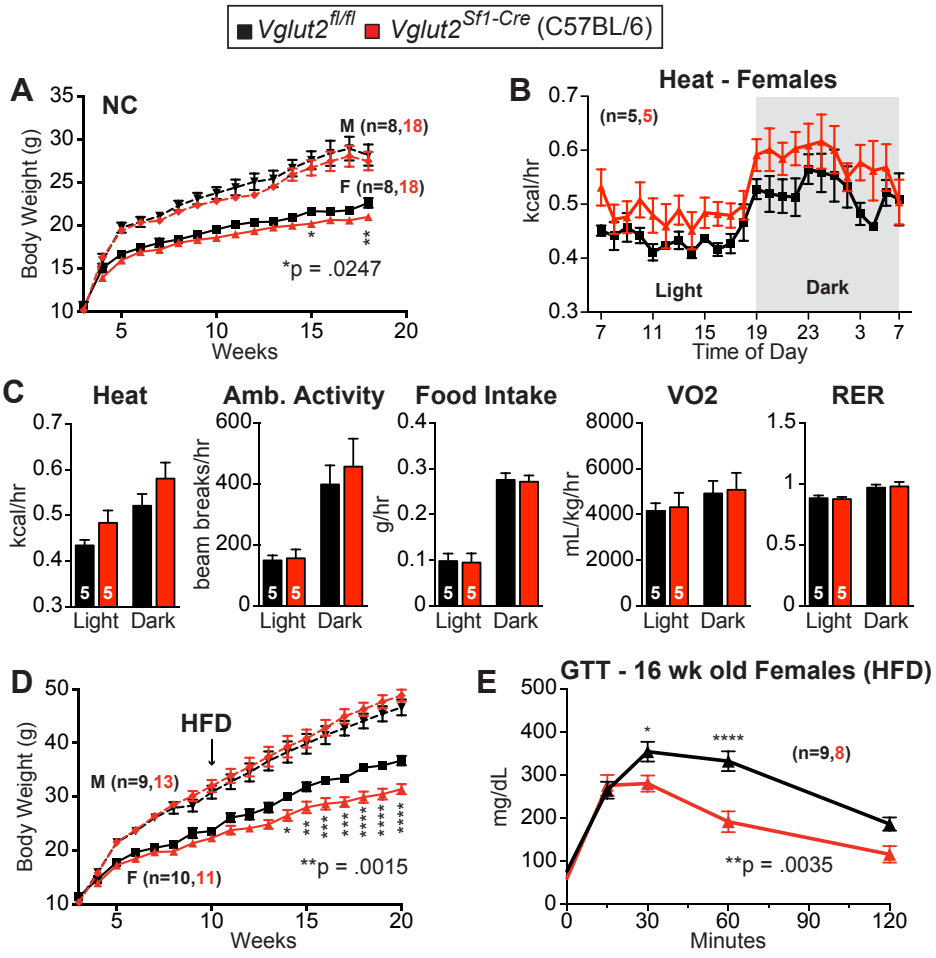

Figure 3: Attenuated Response to HFD in *Vglut2*$^{Sf1\text{-}Cre}$ female mice on a pure C57BL/6 genetic background. A) Weekly body weights of adult male (M) and female (F) *Vglut2*$^{fl/fl}$ and *Vglut2*$^{Sf1\text{-}Cre}$ mice on standard chow (NC). Indicated metabolic parameters measured in adult female *Vglut2*$^{fl/fl}$ and *Vglut2*$^{Sf1\text{-}Cre}$ mice on standard chow using CLAMS chambers. **B)** Hourly heat production during a 24-hour period. **C)** Average hourly heat production, ambulatory activity, food intake, oxygen consumption (VO2), and respiratory exchange ratio (RER) during the same 24-hour period as shown in panel B. **D)** Weekly body weights of male (M) and female (F) *Vglut2*$^{fl/fl}$ and *Vglu2*$^{Sf1\text{-}Cre}$ mice fed HFD beginning at 10 weeks of age (arrow). **E)** Glucose tolerance test in adult (16 wks old) female *Vglut2*$^{fl/fl}$ and *Vglut2*$^{Sf1\text{-}Cre}$ mice on HFD for 6 wks. Data are presented as means ± SEM. For panels A, D, and E, the given *p* values represent the main effect of genotype as determined by 2-way repeated measures ANOVA, and for each time point results from Bonferroni post-test are indicated with * = $p < 0.05$; ** = $p < 0.01$; *** = $p < 0.005$; **** = $p < 0.001$. Number of animals is indicated in each panel.

emotional behavior. Therefore, we asked if learned or innate responses to fear-provoking stimuli are affected in *Vglut2*$^{Sf1\text{-}Cre}$ mice. *Vglut2*$^{Sf1\text{-}Cre}$ mice were subjected to a cued fear-conditioning assay, which links painful stimuli with an auditory cue. While both male and female *Vglut2*$^{Sf1\text{-}Cre}$ mice exhibited normal freezing responses to the aversive foot shock during training, mutant males exhibited a much weaker learned response during testing ($F_{1,23} = 10.06$, $p < 0.005$) (Figure 5A). In contrast, female *Vglut2*$^{Sf1\text{-}Cre}$ mice had normal cued fear responses, with only a significant main effect of conditioning ($F_{2,54} = 204.82$, $p < 0.0001$). Given that female *Vglut2*$^{Sf1\text{-}Cre}$ showed no difference in learned fear, their innate response to the predator fox odor, 2,4,5-trimethyl-3-thiazoline (TMT) was tested. Similar to the cued fear-conditioning, mutant females exhibited normal freezing responses to TMT (Figure 5B).

Finally, we examined the requirement for glutamatergic VMH output in a male-specific social behavior using the resident-intruder assay. Male resident *Vglut2*$^{Sf1\text{-}Cre}$ mice were significantly less aggressive than the *Vglut2*$^{fl/fl}$ controls to a male intruder (Figure 5C). Moreover, among mice that exhibited aggressive behavior, *Vglut2*$^{Sf1\text{-}Cre}$ males attacked far less frequently than their control *Vglut2*$^{fl/fl}$ littermates. Together, these data show that VMH glutamatergic output is essential for context-dependent behaviors in males and anxiety-like behavior in both sexes.

4. DISCUSSION

Here, we created a conditional knockout of VGLUT2 in SF1-expressing cells to examine how excitatory VMH neurotransmission influences metabolism and behavior. Unexpectedly, *Vglut2*$^{Sf1\text{-}Cre}$ mice fail to show increased susceptibility to DIO or impaired glucose homeostasis. Rather we find sex-dependent resistance to DIO that is accompanied by improved glucose tolerance in *Vglut2*$^{Sf1\text{-}Cre}$ females. Conditional loss of VGLUT2 in the VMH also leads to a profound anxiolytic effect in both sexes and reduces aggression and conditioned-fear in males. Our results suggest that glutamatergic signaling in the VMH is largely dispensable for glucose homeostasis, but essential for sex-specific energy storage and for adaptive behavioral responses to anxiety and fear provoking stimuli.

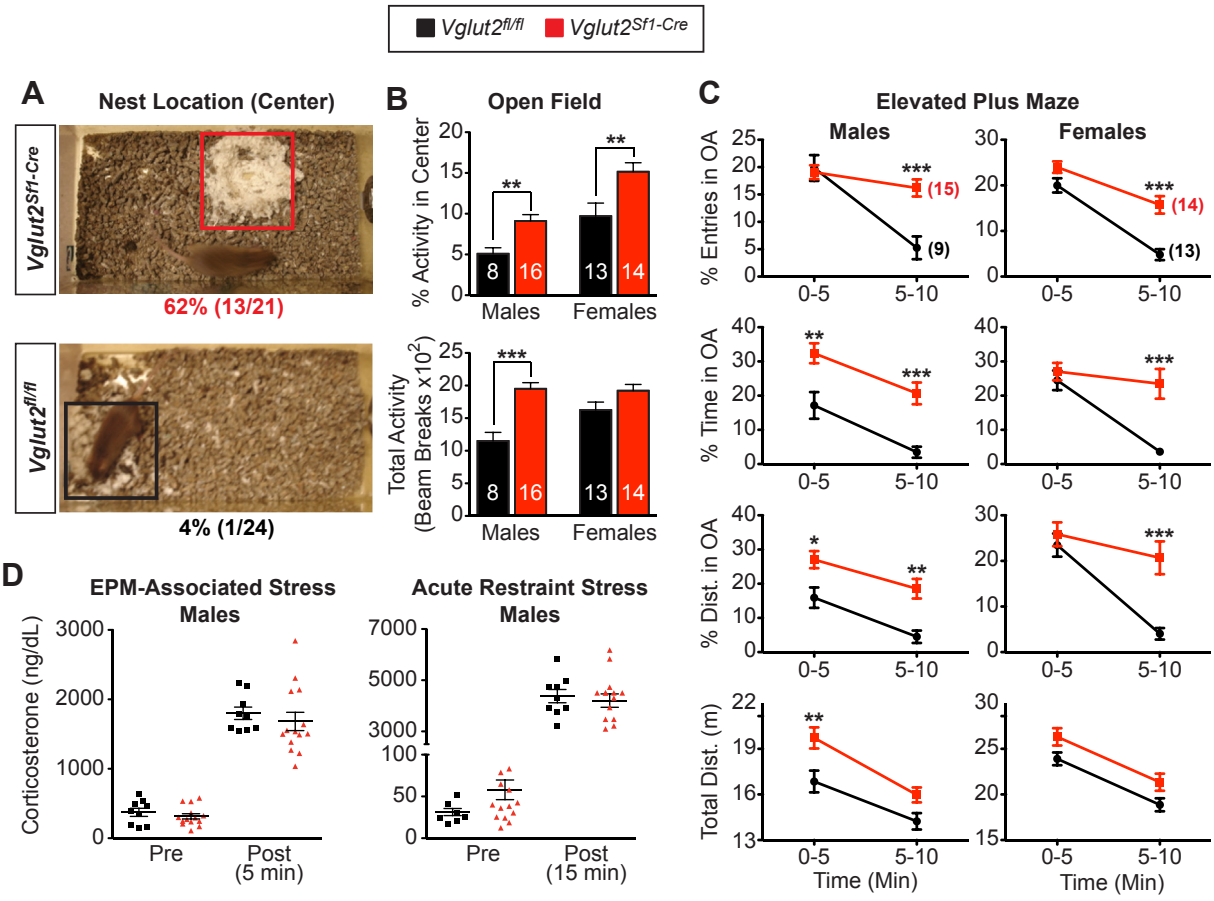

Figure 4: Male and female *Vglu2*$^{Sf1\text{-}Cre}$ mutant mice have reduced levels of anxiety-like behaviors. A) Comparison of nest locations within the home cages of adult *Vglut2*$^{fl/fl}$ and *Vglut2*$^{Sf1\text{-}Cre}$ mice. Percentages reflect the ratio of home cages with centrally located nests built by mutant (top panel) and control (bottom panel) mice. **B)** Activity in center of open field (upper panel, %) and total ambulatory activity (lower panel, beam breaks) measured in adult male and female *Vglut2*$^{fl/fl}$ and *Vglut2*$^{Sf1\text{-}Cre}$ mice in OF test. **C)** Percentage of entries, time spent and distance in the open arm (OA) of the elevated plus-maze as well as total distance in open and closed arms (lower panel) for male and female *Vglut2*$^{fl/fl}$ and *Vglut2*$^{Sf1\text{-}Cre}$ mice. Measurements were binned into two 5-min intervals as graphed. **D)** Serum corticosterone levels measured in adult male *Vglut2*$^{fl/fl}$ and *Vglut2*$^{Sf1\text{-}Cre}$ mice at baseline (Pre) and after (Post) exposure to the indicated stressors. Data are presented as means ± SEM. Statistical significance was determined by unpaired *t*-tests (panel B) or by 2-way repeated measures ANOVA with Bonferroni post-test (panel C). Number of animals is indicated in each panel.

4.1. Blocking VMH glutamatergic output results in female-specific resistance to DIO

The reduced body weight of congenic *Vglut2*$^{Sf1\text{-}Cre}$ C57BL/6 female mice, even on standard chow, demonstrates that glutamatergic output from the VMH is an essential determinant of female energy balance. Although the VMH is a well-known regulator of metabolic homeostasis, this result differs from the increased sensitivity to DIO when leptin signaling in the VMH is ablated using *Sf1-Cre* [11]. These divergent metabolic phenotypes may reflect silencing of excitatory output from all VMH neurons (this study) versus disturbing a single signaling pathway in a subpopulation of VMH neurons. Clearly, the ability to genetically target and lesion different VMH subpopulations is needed for a complete functional understanding of the VMH and energy balance. Indeed, it is often overlooked that use of the *Sf1-Cre*, while specific for the VMH in the brain, is active in other tissues (such as the adrenal gland, pituitary, gonad, and spleen). Thus, it is possible that metabolic disturbances are influenced by depletion of signaling components in other SF-1-expressing tissues outside of the VMH. This issue is less of a problem with *Vglut2*$^{Sf1\text{-}Cre}$ mice. With the exception of rat pituitary gonadotropes [30], the intersection of VGLUT2 and SF-1 expression is largely limited to the VMH. Further, because *Vglut2*$^{Sf1\text{-}Cre}$ mice exhibit normal reproduction, we posit that all metabolic phenotypes observed in *Vglut2*$^{Sf1\text{-}Cre}$ females result primarily from loss of glutamatergic signaling in the VMH.

Our study differs from the previous report that *Vglut2*$^{Sf1\text{-}Cre}$ males and females are heavier when fed a high fat, high sucrose diet, and fail to regulate blood glucose during fasting [15]. One important difference between these two studies is the composition of the HFD. Our HFD contains a lower percent of kcal from carbohydrate and a lower total energy content than the high fat, high sucrose diet utilized by Tong et al. (2007) (20% versus 26% and 5.24 kcal/g versus 5.557 kcal/g, respectively). The source of dietary fat also varies substantially between the two studies (lard versus hydrogenated coconut oil). These nutritional factors could very well lead to differences in DIO outcomes, but fail to adequately account for differences in fasting glucose levels on standard chow. Genetic backgrounds introduced by the Vglut2 floxed allele and the *Sf1-Cre* line are quite different in our study and could potentially affect both DIO [26] and glucose homeostasis by influencing the degree of the hypoglycemic insult needed to reveal a defective counterregulatory response. For our analyses, the *Sf1-Cre* line was backcrossed on to the C57BL/6 background and exhibits robust and specific Cre-mediated recombination throughout the VMH,

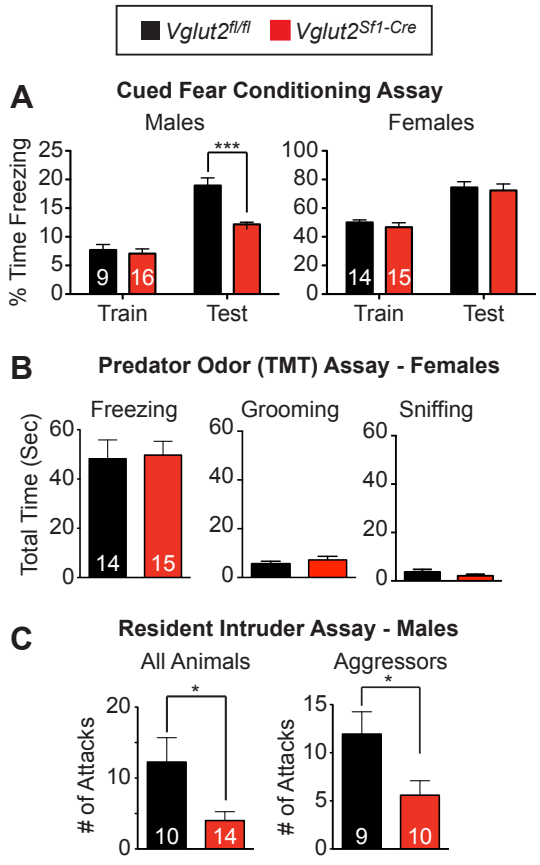

Figure 5: Male *Vglut2*$^{Sf1\text{-}Cre}$ mice exhibit lowered learned fear and social aggression. A) Performance of male and female *Vglut2*$^{fl/fl}$ and *Vglut2*$^{Sf1\text{-}Cre}$ mice in a cued fear conditioning assay that measures learning and memory associated with an aversive stimuli. Fear was quantified as the percent of total time spent freezing immediately after paired presentation of audible tone and foot shock (Train), and 24 h later in response to the conditioned tone (Test). **B)** Time engaged in indicated behaviors during exposure to an olfactory component of fox feces, TMT. **C)** Aggression in male *Vglut2*$^{fl/fl}$ and *Vglut2*$^{Sf1\text{-}Cre}$ mice quantified as the number of attacks toward a resident intruder. Data are shown for all animals tested (All Animals) and only for male mice that displayed aggressive behavior (Aggressors). Data are presented as means ± SEM. Significance was determined by 2-way repeated measures ANOVA with Bonferroni post-test (panel A) or by unpaired *t*-test (panels B, C). Number of animals is indicated in each panel.

including the VMHvl [24]. Thus while VMH neurons are reported to control the counterregulatory response to hypoglycemia [31] and receive input from glucoregulatory CCK-expressing neurons [32], we conclude that under our experimental conditions glutamatergic output from the VMH does not appear to be the primary determinant of glucose homeostasis.

The sex-dependent metabolic phenotype observed in *Vglut2*$^{Sf1\text{-}Cre}$ mice adds to the growing body of literature showing that the VMH is a critical regulator of energy balance and body weight in females. This aspect of VMH function is dependent on estrogen receptor alpha (ERα) in the VMHvl. Reducing ERα expression in the VMHvl [33,34] or the number of ERα-expressing VMHvl neurons [9] leads to female-specific impairment of energy expenditure and increased body weight. In contrast, high estrogen levels or exogenous delivery of estrogen directly to the VMH increases energy expenditure and lowers body weight [35]. Surprisingly, the reduced body weight in the female *Vglut2*$^{Sf1\text{-}Cre}$ mice, the origins of which remain unclear, mimics the metabolic consequence of elevated estrogen signaling. This result undermines the simple assumption that estrogen signaling potentiates VMH neurotransmitter output, suggesting instead that ERα signaling inhibits a circuit that involves glutamatergic VMH output, and that otherwise promotes energy storage. Because this brain region is tightly linked to reproductive behavior [36], we further speculate that estradiol-mediated regulation of glutamatergic VMH neurons in females maximizes fuel reserves in states of overnutrition (HFD) and ultimately improves reproductive fitness in times of undernutrition.

4.2. Glutamatergic output from the VMH controls innate and learned behavior

Our data also reveal that glutamatergic VMH output contributes greatly to excitatory signals and neural circuits that modulate emotional behaviors, including those associated with anxiety-like behavior, fear, and sex-specific social behaviors. Indeed, we find that glutamatergic signaling from the VMH is required for male aggression. Ablating VMHvl neurons dramatically inhibits male aggressive behaviors [21]. Conversely, artificially activating VMHvl neurons triggers male aggressive behaviors [20]. As predicted from these studies, we find that disrupting the excitatory VMH output decreases the amount and extent of attack behavior when male *Vglut2*$^{Sf1\text{-}Cre}$ mice are presented with a resident intruder. That *Vglut2*$^{Sf1\text{-}Cre}$ males, but not females, exhibit lowered behavioral responses to a conditioned fear-provoking stimulus and exhibit increased novelty-associated locomotion but have no metabolic phenotype expand on the theme that the VMH mediates important sex-differences. Moreover, these data imply that neural circuits controlling fear and anxiety-like behaviors and metabolic responses are not tightly coupled.

Similar to the anxiolytic phenotype described here, acute, postnatal ablation of *Sf1*-positive neurons, which would also extinguish VMH glutamatergic output, significantly decreases anxiety-like behavior in the EPM [37]. The anxiolytic phenotype observed in *Vglut2*$^{Sf1\text{-}Cre}$ mice differs from the anxiogenic phenotype noted in *Sf1*$^{Nestin\text{-}Cre}$ mutants. However, the latter genetic lesion not only eliminates SF-1 in the VMH, but also disrupts the overall integrity of the VMH. Taken together, we conclude that the differences in anxiety-like behaviors observed in *Vglut2*$^{Sf1\text{-}Cre}$ and *Sf1*$^{Nestin\text{-}Cre}$ result from impaired VMH neuronal function versus disrupted VMH organization, respectively. We further demonstrate that circulating corticosterone, which mediates the physiological response to stress upon activation of the HPA axis is unaffected in *Vglut2*$^{Sf1\text{-}Cre}$ mutants. Interestingly, *Sf1*$^{Nestin\text{-}Cre}$ mutants exhibit normal circadian fluctuations in corticosterone [18]. Thus, the role of the VMH in anxiety-like behavior appears distinct from regulation of the HPA axis

The periaqueductal grey (PAG) is a prominent downstream target of VMH projections [21,24,38], and regulates behaviors associate with anxiety and fear in response to glutamate. Consistent with the anxiolytic effect observed in mutant mice that have lost excitatory VMH output, delivering a glutamate receptor antagonist, 2-amino-7-phosphonoheptanoic acid, directly to the PAG in rats decreases anxiety-like behavior in the EPM [39]. Silencing VMH or PAG activity in mice using designer receptors exclusively activated by designer drugs (DREADDs) also impairs behavioral responses to fear-inducing stimuli, such as a predator or an aggressive conspecific [17]. Local application of a glutamate receptor agonist, N-methyl-D-aspartate, to the PAG in rats increases anxiety-like behavior in the EPM [40]. Collectively, we suggest that glutamatergic output from the VMH provides at least some of the excitatory input to the PAG that drives emotional behaviors associated with anxiety and/or fear.

Results from our behavioral assays indicate that not all responses to fearful stimuli are disrupted after inhibiting VMH glutamate release. For

instance, female mutant and control mice display equivalent levels of freezing to a predator odor, and both male and female *Vglut2*$^{Sf1\text{-}Cre}$ mice had normal freezing responses to foot shock during fear conditioning. However, during testing, male *Vglut2*$^{Sf1\text{-}Cre}$ mice had a weaker conditioned response, indicating impairment in the formation or recall of the association between auditory tone and foot shock. Together, the lack of a uniform response to different anxiogenic and fear-provoking stimuli in *Vglut2*$^{Sf1\text{-}Cre}$ mutants is broadly consistent with the idea that distinct neural circuits mediate behavioral responses to different sources of anxiety and/or fear [41].

4.3. Conclusions

In summary, our study establishes that excitatory glutamatergic output from the VMH is required for optimal energy storage in females and appropriate behavioral responses to novel or fear-evoking stimuli in both sexes. The phenotypes of *Vglut2*$^{Sf1\text{-}Cre}$ mice reported here are consistent with emerging evidence that the VMH, specifically the VMHvl, regulates sex-dependent metabolic responses and social behaviors. Clearly, additional work is needed to define the precise anatomical and molecular pathways in the VMH needed to generate the complex emotional and metabolic responses associated with this neuroendocrine region.

ACKNOWLEDGMENTS

We thank Drs. S. Correa, E. Unger and C. Herber for careful reading of the manuscript and J. Leung and D. Newstrom for technical assistance in this project. Data for this paper was acquired using the Nikon Imaging Center at UCSF/QB3, the Gladstone Neural Behavioral Core and the Mouse Metabolic Core funded by UCSF DERC (NIDDK P30 DK063720). Support for the work includes NIDDK-1K08DK076721 and Lawson Wilkins Pediatric Endocrine Society Clinical Scholar Awards to C.C.C, NINDS-R01NS049488 and R01NS083872 to N.M.S., and NIH-NIDA K01DA026504 to T.S.H., a CCRC award to H.A.I to support W.C.K., funding from the UCSF Diabetes Family Fund, AHA Grant-in-Aid 13GRNT16120004, and NIDDK-R01DK09972 to H.A.I.

CONFLICT OF INTEREST

None declared.

APPENDIX A. SUPPLEMENTARY DATA

Supplementary data related to this article can be found at http://dx.doi.org/10.1016/j.molmet.2015.09.001.

REFERENCES

[1] Kurrasch, D.M., Cheung, C.C., Lee, F.Y., Tran, P.V., Hata, K., Ingraham, H.A., 2007. The neonatal ventromedial hypothalamus transcriptome reveals novel markers with spatially distinct patterning. Journal of Neuroscience 27(50): 13624–13634.

[2] Ziegler, D.R., Cullinan, W.E., Herman, J.P., 2002. Distribution of vesicular glutamate transporter mRNA in rat hypothalamus. Journal of Comparative Neurology 448(3):217–229.

[3] Fremeau Jr., R.T., Troyer, M.D., Pahner, I., Nygaard, G.O., Tran, C.H., Reimer, R.J., et al., 2001. The expression of vesicular glutamate transporters defines two classes of excitatory synapse. Neuron 31(2):247–260.

[4] Fu, L.Y., 2008. van den Pol AN. Agouti-related peptide and MC3/4 receptor agonists both inhibit excitatory hypothalamic ventromedial nucleus neurons. Journal of Neuroscience 28(21):5433–5449.

[5] Sternson, S.M., Shepherd, G.M., Friedman, J.M., 2005. Topographic mapping of VMH–> arcuate nucleus microcircuits and their reorganization by fasting. Nature Neuroscience 8(10):1356–1363.

[6] Kim, K.W., Zhao, L., Donato Jr., J., Kohno, D., Xu, Y., Elias, C.F., et al., 2011. Steroidogenic factor 1 directs programs regulating diet-induced thermogenesis and leptin action in the ventral medial hypothalamic nucleus. Proceedings of the National Academy of Sciences of the United States of America 108(26): 10673–10678.

[7] Tran, P.V., Akana, S.F., Malkovska, I., Dallman, M.F., Parada, L.F., Ingraham, H.A., 2006. Diminished hypothalamic bdnf expression and impaired VMH function are associated with reduced SF-1 gene dosage. Journal of Comparative Neurology 498(5):637–648.

[8] Majdic, G., Young, M., Gomez-Sanchez, E., Anderson, P., Szczepaniak, L.S., Dobbins, R.L., et al., 2002. Knockout mice lacking steroidogenic factor 1 are a novel genetic model of hypothalamic obesity. Endocrinology 143(2):607–614.

[9] Correa, S.M., Newstrom, D.W., Warne, J.P., Flandin, P., Cheung, C.C., Lin-Moore, A.T., et al., 2015. An estrogen-responsive module in the ventromedial hypothalamus selectively drives sex-specific activity in females. Cell Reports 10(1):62–74.

[10] Xu, Y., Hill, J.W., Fukuda, M., Gautron, L., Sohn, J.W., Kim, K.W., et al., 2010. PI3K signaling in the ventromedial hypothalamic nucleus is required for normal energy homeostasis. Cell Metabolism 12(1):88–95.

[11] Dhillon, H., Zigman, J.M., Ye, C., Lee, C.E., McGovern, R.A., Tang, V., et al., 2006. Leptin directly activates SF1 neurons in the VMH, and this action by leptin is required for normal body-weight homeostasis. Neuron 49(2):191–203.

[12] Bingham, N.C., Anderson, K.K., Reuter, A.L., Stallings, N.R., Parker, K.L., 2008. Selective loss of leptin receptors in the ventromedial hypothalamic nucleus results in increased adiposity and a metabolic syndrome. Endocrinology 149(5):2138–2148.

[13] Chiappini, F., Catalano, K.J., Lee, J., Peroni, O.D., Lynch, J., Dhaneshwar, A.S., et al., 2014. Ventromedial hypothalamus-specific Ptpn1 deletion exacerbates diet-induced obesity in female mice. Journal of Clinical Investigation 124(9):3781–3792.

[14] Klöckener, T., Hess, S., Belgardt, B.F., Paeger, L., Verhagen, L.A., Husch, A., et al., 2011. High-fat feeding promotes obesity via insulin receptor/PI3K-dependent inhibition of SF-1 VMH neurons. Nature Neuroscience 14(7): 911–918.

[15] Tong, Q., Ye, C., McCrimmon, R.J., Dhillon, H., Choi, B., Kramer, M.D., et al., 2007. Synaptic glutamate release by ventromedial hypothalamic neurons is part of the neurocircuitry that prevents hypoglycemia. Cell Metabolism 5(5): 383–393.

[16] Motta, S.C., Goto, M., Gouveia, F.V., Baldo, M.V., Canteras, N.S., Swanson, L.W., 2009. Dissecting the brain's fear system reveals the hypothalamus is critical for responding in subordinate conspecific intruders. Proceedings of the National Academy of Sciences of the United States of America 106(12):4870–4875.

[17] Silva, B.A., Mattucci, C., Krzywkowski, P., Murana, E., Illarionova, A., Grinevich, V., et al., 2013. Independent hypothalamic circuits for social and predator fear. Nature Neuroscience 16(12):1731–1733.

[18] Zhao, L., Kim, K.W., Ikeda, Y., Anderson, K.K., Beck, L., Chase, S., et al., 2008. Central nervous system-specific knockout of steroidogenic factor 1 results in increased anxiety-like behavior. Molecular Endocrinology 22(6):1403–1415.

[19] Kruk, M.R., Van der Poel, A.M., Meelis, W., Hermans, J., Mostert, P.G., Mos, J., et al., 1983. Discriminant analysis of the localization of aggression-inducing electrode placements in the hypothalamus of male rats. Brain Research 260(1):61–79.

[20] Lin, D., Boyle, M.P., Dollar, P., Lee, H., Lein, E.S., Perona, P., et al., 2011. Functional identification of an aggression locus in the mouse hypothalamus. Nature 470(7333):221–226.

[21] Yang, C.F., Chiang, M.C., Gray, D.C., Prabhakaran, M., Alvarado, M., Juntti, S.A., et al., 2013. Sexually dimorphic neurons in the ventromedial hypothalamus govern mating in both sexes and aggression in males. Cell 153(4):896–909.

[22] Hnasko, T.S., Chuhma, N., Zhang, H., Goh, G.Y., Sulzer, D., Palmiter, R.D., et al., 2010. Vesicular glutamate transport promotes dopamine storage and glutamate corelease in vivo. Neuron 65(5):643–656.

[23] Moechars, D., Weston, M.C., Leo, S., Callaerts-Vegh, Z., Goris, I., Daneels, G., et al., 2006. Vesicular glutamate transporter VGLUT2 expression levels control quantal size and neuropathic pain. Journal of Neuroscience 26(46):12055–12066.

[24] Cheung, C.C., Kurrasch, D.M., Liang, J.K., Ingraham, H.A., 2013. Genetic labeling of steroidogenic factor-1 (SF-1) neurons in mice reveals ventromedial nucleus of the hypothalamus (VMH) circuitry beginning at neurogenesis and development of a separate non-SF-1 neuronal cluster in the ventrolateral VMH. Journal of Comparative Neurology 521(6):1268–1288.

[25] Stuber, G.D., Hnasko, T.S., Britt, J.P., Edwards, R.H., Bonci, A., 2010. Dopaminergic terminals in the nucleus accumbens but not the dorsal striatum corelease glutamate. Journal of Neuroscience 30(24):8229–8233.

[26] Montgomery, M.K., Hallahan, N.L., Brown, S.H., Liu, M., Mitchell, T.W., Cooney, G.J., et al., 2013. Mouse strain-dependent variation in obesity and glucose homeostasis in response to high-fat feeding. Diabetologia 56(5):1129–1139.

[27] Collins, S., Martin, T.L., Surwit, R.S., Robidoux, J., 2004. Genetic vulnerability to diet-induced obesity in the C57BL/6J mouse: physiological and molecular characteristics. Physiology & Behavior 81(2):243–248.

[28] Crawley, J.N., 2008. Behavioral phenotyping strategies for mutant mice. Neuron 57(6):809–818.

[29] Rodgers, R.J., Johnson, N.J., 1995. Factor analysis of spatiotemporal and ethological measures in the murine elevated plus-maze test of anxiety. Pharmacology Biochemistry & Behavior 52(2):297–303.

[30] Hrabovszky, E., Kallo, I., Turi, G.F., May, K., Wittmann, G., Fekete, C., et al., 2006. Expression of vesicular glutamate transporter-2 in gonadotrope and thyrotrope cells of the rat pituitary. Regulation by estrogen and thyroid hormone status. Endocrinology 147(8):3818–3825.

[31] Borg, M.A., Sherwin, R.S., Borg, W.P., Tamborlane, W.V., Shulman, G.I., 1997. Local ventromedial hypothalamus glucose perfusion blocks counterregulation during systemic hypoglycemia in awake rats. Journal of Clinical Investigation 99(2):361–365.

[32] Garfield, A.S., Shah, B.P., Madara, J.C., Burke, L.K., Patterson, C.M., Flak, J., et al., 2014. A parabrachial-hypothalamic cholecystokinin neurocircuit controls counterregulatory responses to hypoglycemia. Cell Metabolism 20(6):1030–1037.

[33] Xu, Y., Nedungadi, T.P., Zhu, L., Sobhani, N., Irani, B.G., Davis, K.E., et al., 2011. Distinct hypothalamic neurons mediate estrogenic effects on energy homeostasis and reproduction. Cell Metabolism 14(4):453–465.

[34] Musatov, S., Chen, W., Pfaff, D.W., Mobbs, C.V., Yang, X.J., Clegg, D.J., et al., 2007. Silencing of estrogen receptor alpha in the ventromedial nucleus of hypothalamus leads to metabolic syndrome. Proceedings of the National Academy of Sciences of the United States of America 104(7):2501–2506.

[35] Martinez de Morentin, P.B., Gonzalez-Garcia, I., Martins, L., Lage, R., Fernandez-Mallo, D., Martinez-Sanchez, N., et al., 2014. Estradiol regulates brown adipose tissue thermogenesis via hypothalamic AMPK. Cell Metabolism 20(1):41–53.

[36] Ogawa, S., Eng, V., Taylor, J., Lubahn, D.B., Korach, K.S., Pfaff, D.W., 1998. Roles of estrogen receptor-alpha gene expression in reproduction-related behaviors in female mice. Endocrinology 139(12):5070–5081.

[37] Kunwar, P.S., Zelikowsky, M., Remedios, R., Cai, H., Yilmaz, M., Meister, M., et al., 2015. Ventromedial hypothalamic neurons control a defensive emotion state. Elife, 4.

[38] Canteras, N.S., Simerly, R.B., Swanson, L.W., 1994. Organization of projections from the ventromedial nucleus of the hypothalamus: a Phaseolus vulgaris-leucoagglutinin study in the rat. Journal of Comparative Neurology 348(1):41–79.

[39] Guimaraes, F.S., Carobrez, A.P., De Aguiar, J.C., Graeff, F.G., 1991. Anxiolytic effect in the elevated plus-maze of the NMDA receptor antagonist AP7 microinjected into the dorsal periaqueductal grey. Psychopharmacology (Berl) 103(1):91–94.

[40] Miguel, T.T., Nunes-de-Souza, R.L., 2008. Anxiogenic-like effects induced by NMDA receptor activation are prevented by inhibition of neuronal nitric oxide synthase in the periaqueductal gray in mice. Brain Research 1240:39–46.

[41] Gross, C.T., Canteras, N.S., 2012. The many paths to fear. Nature Reviews Neuroscience 13(9):651–658.

